*Original Research Paper*

# Antibacterial and osseointegration evaluation of silver ion-implanted orthopaedic implants

Journal of Micromanufacturing
1–12
© The Author(s) 2025
Article reuse guidelines:
in.sagepub.com/journals-permissions-india
DOI: 10.1177/25165984251382378
journals.sagepub.com/home/jmf
Sage

**Sara Hawi[1], Saurav Goel[2,3,4], Jaume Caro[5], Raül Bonet[5], Jordi Orrit-Prat[5], Jose L Endrino[6], Oliver Pearce[7] and Wayne Nishio[8]**

## Abstract

This study investigates the efficacy of silver ion-implanted or impregnated freeform surfaces of locking compression plates (LCPs) for orthopaedic applications, specifically targeting the prevention of surgical site infections without affecting the future removability of fracture fixation devices. Using stainless-steel LCPs as a testbed, we explored the antibacterial activity of silver-implanted LCP plates against *Staphylococcus aureus* as well as assessed the biocompatibility through osteoblast-like cell behaviour.

Silver-ion-implanted LCPs demonstrated a 72% reduction in bacterial adhesion compared to controls ($p < .01$, Cohen's $d = 8.2$), along with a 4.5-fold increase in the proportion of dead bacteria ($p < .001$, Cohen's $d = 10.6$), although this efficacy was lower than that reported for similar ion dosages in the literature, likely due to the complexities of non-planar geometries. Furthermore, the silver-treated surfaces influenced osteoblast-like cells to exhibit a >60% reduction in attachment compared to untreated controls, with cells showing predominantly rounded morphology, an outcome beneficial for fracture fixation plates intended for eventual removal, as it discourages osseointegration. Our findings revealed the promising antimicrobial potential of silver ions as an excellent agent for the improved antibacterial performance of the LCP surfaces for fracture fixation, marking a departure from the traditional focus on permanent implant osseointegration. A key novelty of this work is the application of silver ion implantation to full-scale, geometrically complex orthopaedic implants, as opposed to the flat samples typically used in prior studies. The observed discrepancies between our results on freeform surfaces and theoretical predictions/experimental data from flat samples necessitate a deeper investigation into the influence of complex surface geometries. These results underscore the critical need to refine both our models and implantation processes to account for the effects of complex surface topography.

## Keywords

Antibacterial, silver implantation, biotesting, osseointegration

**Received** 02 July 2025; **revised** 03 September 2025; **accepted** 09 September 2025

## Introduction

Orthopaedic implants serve as artificial joint replacements and as plates and screws for fracture fixation when natural joints and bone deteriorate or fail under mechanical stress. However, not all implants necessitate osseointegration, such as forearm plates that assist in fractured bone fixation,[1] which makes infection control a higher priority. However, as their surfaces inherently lack bactericidal properties, they often serve as a breeding ground for bacterial adhesion, proliferation, and biofilm formation. This leads to potential risks of infection, a problem observed especially in non-cemented implants.[2] In orthopaedic care, the incidence of fracture-related infections presents a significant challenge, with rates varying between 1.3% and 9% across different implant sites. This variability highlights the complexities of managing infections in a field where outcomes can be critically influenced by numerous factors. Illustratively, a study from one of Europe's busiest trauma centres reported 330 infection episodes in 294 patients over six years,[3] underscoring the prevalence and the difficulty of infection control in high-volume

[1]Cranfield University, Cranfield, UK
[2]China Beacons of Excellence Research and Innovation Institute (CBI), University of Nottingham Ningbo China (UNNC), Ningbo, China
[3]London South Bank University, London, UK
[4]University of Petroleum and Energy Studies, Dehradun, Uttarakhand, India
[5]Eurecat, Centre Tecnològic de Catalunya, Manresa, Spain
[6]Universidad Loyola Andalucía, Sevilla, Spain
[7]Milton Keynes University Hospital, Milton Keynes, UK
[8]Cardiff University, Cardiff, UK

**Corresponding author:**
Saurav Goel, London South Bank University, London, SE10AA, UK.
E-mail: goeLs@Lsbu.ac.uk

settings. Iliaens et al.[4] shed light on the economic burden, noting that the direct costs associated with treating these infections are eight times higher than for patients without infections. Additionally, they highlight the profound impact on quality of life, with a marked decrease in physical function among those affected. The cumulative effect of these issues emphasises that the repercussions of fracture-related infections extend far beyond financial costs, affecting patient health and well-being deeply.

Traditional methods of preventing biomaterial-bound bacterial infections largely rely on antibiotics. However, the rise of antibiotic resistance necessitates alternative solutions. Researchers have focused on understanding bacterial adhesion and developing surfaces that deter bacterial adhesion and growth. Incorporation of antibacterial elements such as silver (Ag), copper (Cu), and zinc (Zn) has shown promising results due to their ability to interact with bacterial cellular processes and cause irreversible DNA damage to bacteria.[5,6]

Silver impregnation, because of its dual antibacterial and osteogenic properties[7] has gained attention in both research and industrial applications.[5] Companies like Accentus Medical Ltd have introduced products like Agluna®, which leverage silver's antibacterial properties.[6] Despite the progress, these solutions still face challenges with implementation, especially concerning osseointegration,[8,9] largely due to issues like coating delamination. Therefore, alternative methods like ion implantation are being explored.

Ion implantation is a sophisticated surface engineering technique that utilises ionised atomic species accelerated at high energy in a vacuum environment. This method serves as a means of immobilising accelerated particles on the surface of a substrate. Unlike conventional surface coatings, this process enables the atoms to penetrate the substrate at the subsurface level. This unique characteristic eliminates the risk of delamination, an issue often encountered with traditional surface coatings. It also allows for the preservation of the substrate's bulk properties,[10] making it advantageous for a variety of applications.

Among the various ion implantation methods, Plasma Immersion Ion Implantation (PIII) is particularly noteworthy.[11–16] It stands out for its versatility and effectiveness in modifying surfaces with complex geometries, eliminating the line-of-sight restrictions seen in other implantation techniques. PIII operates in a specialised vacuum chamber, equipped with a workpiece stage, plasma source, and high-voltage pulse modulator.[17] During the process, the samples are submerged in high-density plasma and subjected to a high-voltage negative pulse, facilitating the ion bombardment towards the substrate surface. This results in a thin, implanted sublayer typically in the order of tens of nanometres.

This technique can be further tailored by adjusting the implantation parameters to control ion concentration and depth, offering exceptional control over the modified layer. Moreover, PIII can be used in conjunction with different plasma ion sources like Metal Vapour Vacuum Arc (MEVVA), Electron Cyclotron Resonance (ECR), and Kaufman among others.[17] One particularly exciting application is the implantation of biocidal elements like Ag, Cu, or Zn, which can be used for the creation of antibacterial surfaces. PIII even allows the integration of these biocidal elements with bioactive ones such as Ca and Mg, paving the way for more comprehensive biomedical applications.

Given these advantages and the level of control offered by PIII, it opens a new frontier in the creation of antibacterial biomaterials. While the incorporation of antimicrobial agents into various medical products is not novel, what is relatively new is the surface engineering of biomaterials themselves to imbue them with antibacterial properties.

Although antimicrobial materials have long been used in disinfecting solutions and wound dressings[18,19] their incorporation into the very surfaces of biomedical implants has only recently gained considerable attention. Among these, silver and silver nanoparticles (Ag NPs) stand out. They are increasingly being employed due to their high reactivity and expansive active surface area. Under environmental and physiological conditions, Ag NPs oxidise and release $Ag^+$ ions, which are theorised to be the hub of the bactericidal action of silver by disrupting bacterial membranes and reducing their viability.[20–22] This happens through strong interactions between the ionic $Ag^+$ and thiol groups of cystine residues of proteins present in bacterial cell walls.[24] While higher dosages of implanted Ag have been shown to yield greater bactericidal effects,[17,20] recent research highlights the importance of optimising the concentration of silver to achieve antibacterial activity without cytotoxic effects.[23] This balance is particularly relevant for Ag ion-implanted substrates, which have also demonstrated favourable outcomes in osseointegration and cytocompatibility.[24]

*Staphylococcus aureus (S. aureus)* is of particular interest in this work as it is an opportunistic pathogen associated with the majority of orthopaedic surgical site infections, community and hospital-acquired infections.[25,26]

This research focuses on the chemical modification of orthopaedic biomedical surfaces, specifically locking compression plates (LCPs). It explores the potential of ion implantation, which is emerging as a promising avenue to tackle bacterial infections related to orthopaedic applications.

While the existing body of literature robustly demonstrates the efficacy of silver ion implantation in enhancing antibacterial properties, a significant limitation persists: the vast majority of these studies are conducted on flat, polished coupons of implant materials.[24,27] This approach, while valuable for foundational research, fails to capture the challenges and realities of treating commercial orthopaedic devices, which feature intricate screws holes, curvatures, and non-line-of-sight surfaces. Therefore, the primary novelty of this research lies in its focus on applying silver PIII to full-scale, commercial LCPs with complex freeform geometries. This work bridges the gap between idealised laboratory studies and real-world clinical application, critically evaluating how complex

topography influences antibacterial efficacy and cellular response.

In the subsequent sections, a comparative analysis is provided between unmodified LCP samples and those subjected to silver ion implantation. A significant novelty of this research lies in the application of these techniques to full-scale orthopaedic implants, a perspective currently underrepresented in the literature. The study scrutinises the effects of silver ion implantation on bacterial attachment, cell morphology, and overall antibacterial performance, aiming to yield valuable insights about the effectiveness of this promising approach in real-world settings.

## Methods

### *Silver Ion implantation*

Stryker orthopaedic (Michigan, US) implant samples, including LCPs composed of stainless steel, spiral blades composed of titanium aluminium niobium alloy and the femoral component of a knee replacement implant composed of cobalt-chromium alloy (Figure 1), acquired from Milton Keynes University Hospital (MKUH), were subsequently processed with silver ion implantation.

Silver implantation processes for orthopaedic implant parts were performed in a pulsed filtered cathodic vacuum arc system (PFCVA-450, Plasma Technology Limited, Hong Kong). To reduce the incorporation of detrimental microparticles into the samples, this system is equipped with two pulsed filtered cathodic arc sources, where the generated arc plasmas are directed into the vacuum chamber by an electromagnetic field applied to the curved ducts. The samples were positioned in the centre of the chamber (240 mm away from the exit of the filtered duct), and they were negatively biased to a high pulsed voltage. More details of this equipment can be found elsewhere.[31] A schematic and picture of the system are presented in Figure 2.

The implantation parameters, including ion dose, energy and substrate temperature, were guided by the review of the existing literature to achieve a surface concentration of silver that is biocidal yet minimises potential cytotoxic effects.[23,24] A dose of approximately $4.0 \times 10^{17}$ ions/cm$^2$ was targeted since this range has been previously shown to confer significant antibacterial properties against *S. aureus* on metallic substrates without completely inhibiting mammalian cell function.[24,32] An implantation energy of −20 kV was selected to ensure sufficient ion penetration into the sub-surface region (tens of nanometres, as confirmed by Stopping and Range of Ions in Matter (SRIM) simulations shown later in Figure 4), creating a durable reservoir of silver ions that is less susceptible to wear than a superficial coating.[10] A substrate temperature of 175°C was maintained to facilitate the diffusion and incorporation of implanted ions without inducing undesirable phase transformations or thermal stress in the stainless-steel substrate, which has a much higher annealing temperature.[10]

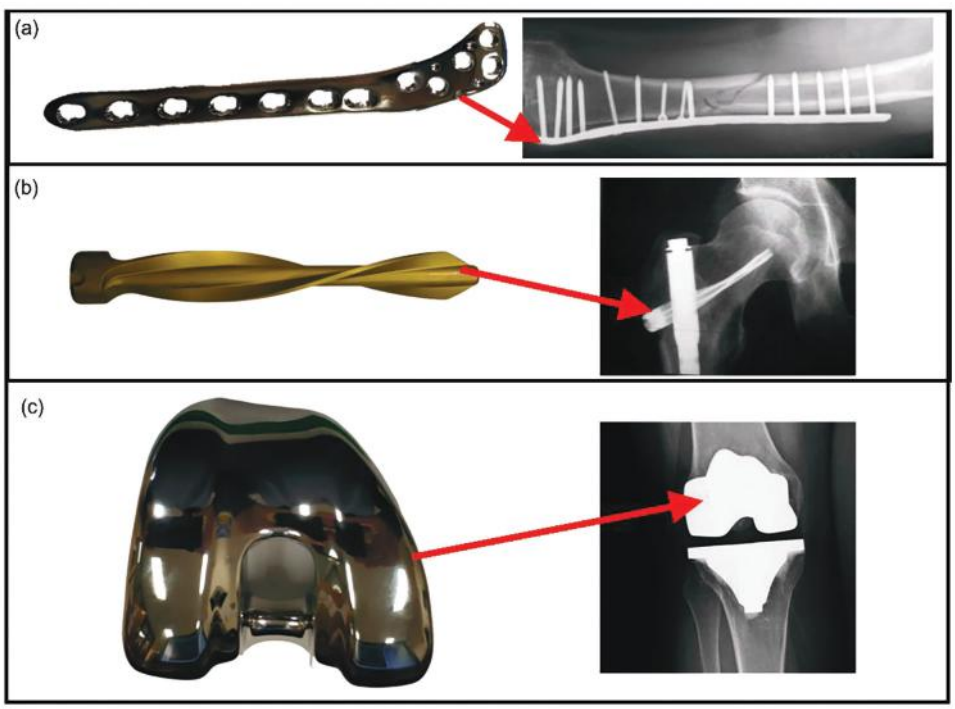



**Figure 1.** (a) Locking compression plate (stainless steel) and its application,[28] (b) spiral blade (titanium niobium alloy) and its application[29] and (c) knee replacement femoral component (cobalt chromium alloy) and its application.[30]

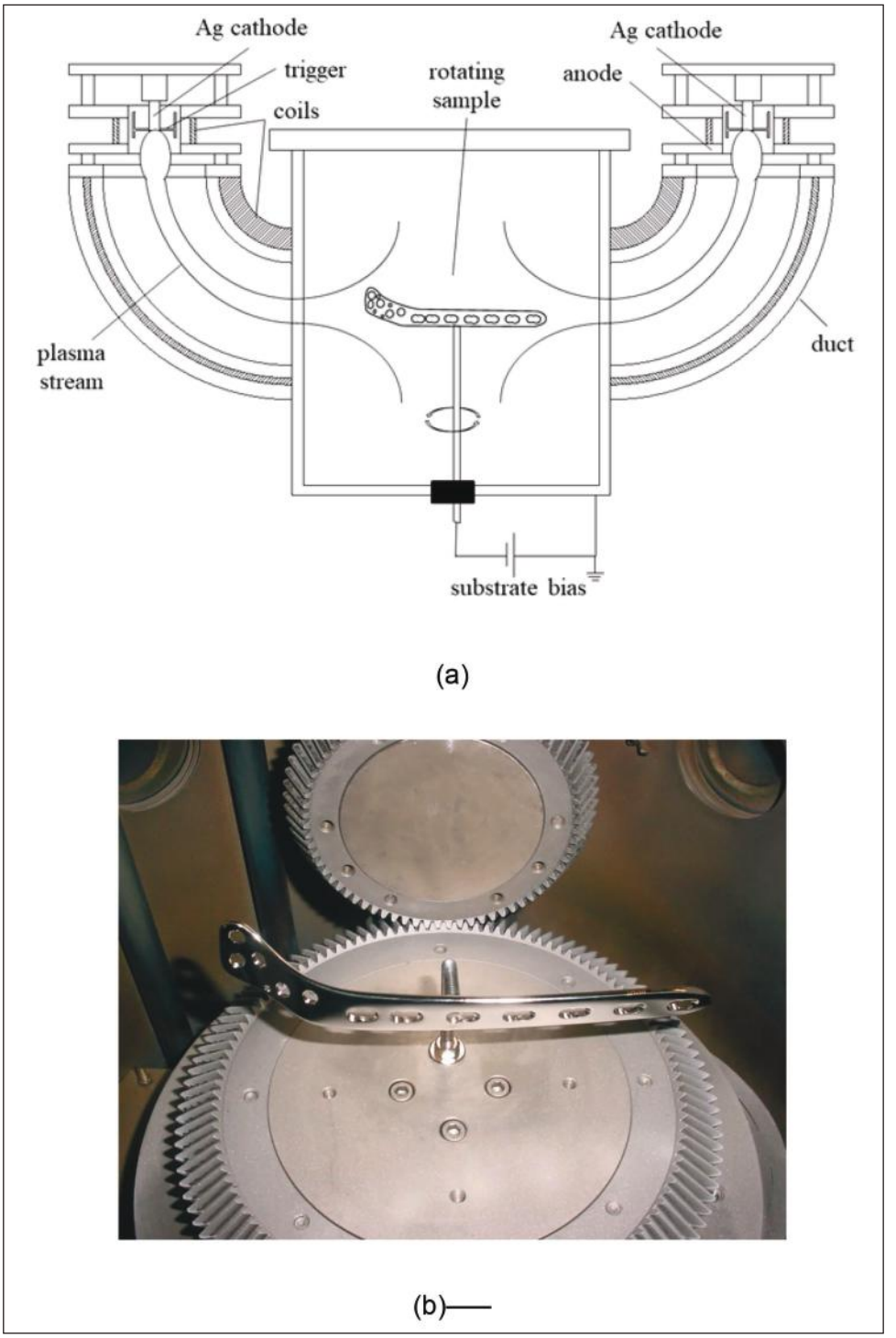



**Figure 2.** (a) Schematic of the pulsed filtered cathodic vacuum arc system. (b) Placement of the locking compression plate (LCP) prosthesis on the rotating sample holder.

Two high-purity silver cathodes (99.95%) were co-evaporated on a rotating sample. The cathodes were ignited at 50 V, using a pulse duration of 450 μs at a frequency of 7 Hz, generating a mean arc current of about 0.17 A. An argon flow of 2 sccm was introduced through each arc source. The implantation process was carried out at a working pressure of 0.03 Pa, for 60 min and at 175 ºC substrate temperature. The samples were biased to a pulsed potential of −20 kV (7 Hz, 600 μs). Under these conditions, the bias current was ~34 mA, corresponding to an ion dose of approximately $4.0 \times 10^{17}$ ions/cm².

All fabricated samples were cleaned by sonication with acetone for 15 min, sonication with isopropanol for 10 min,

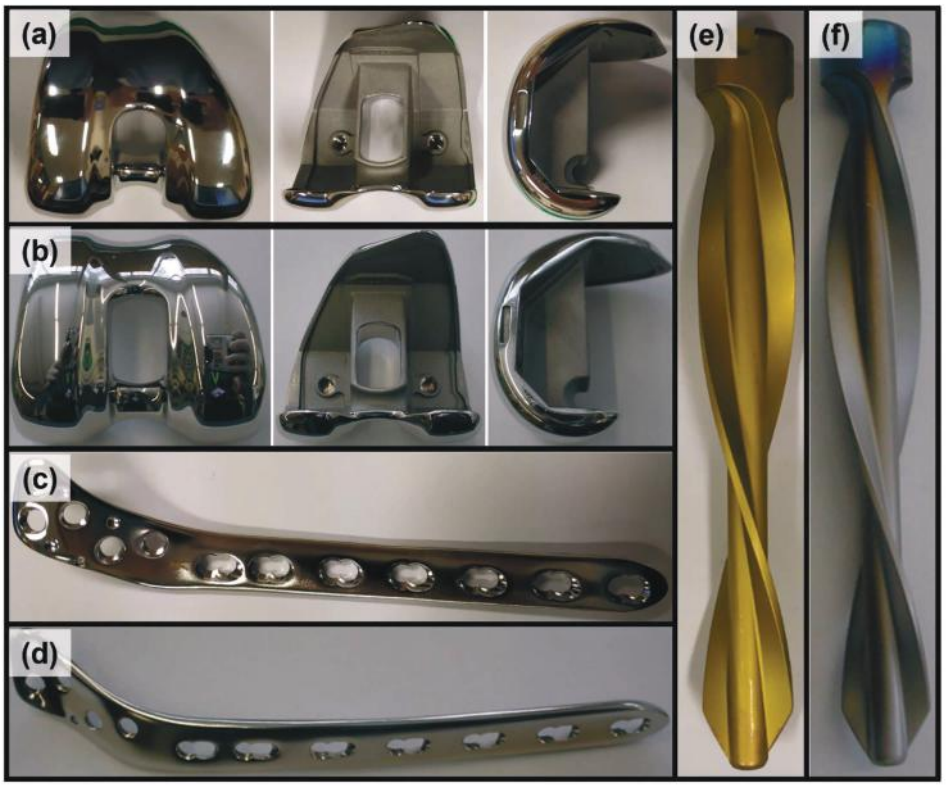



**Figure 3.** Knee replacement femoral component (a) before and (b) after surface treatment. Locking compression plate (c) before and (d) after surface treatment. Spiral blade (e) before and (f) after surface treatment.

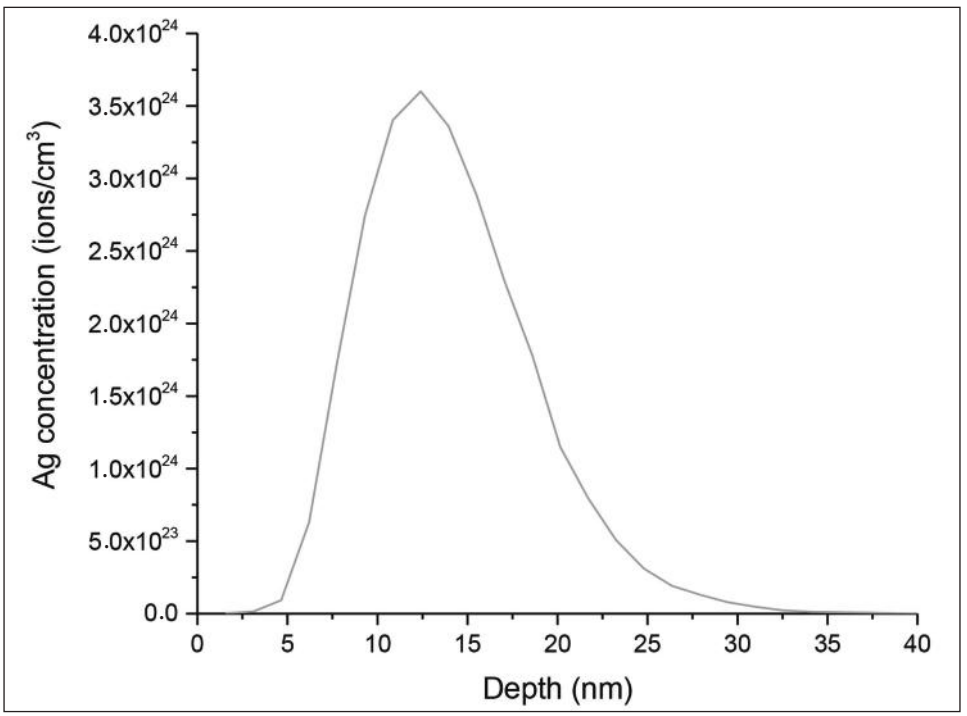



**Figure 4.** SRIM-simulated silver ion concentration versus implantation depth in stainless steel. The curve represents an idealised depth profile generated under assumptions of flat geometry, normal ion incidence and homogeneous material composition. These results should be interpreted as a theoretical reference; real freeform implant geometries may deviate substantially due to angular incidence, shadowing, and surface roughness effects. Direct experimental characterisation is required in future work to validate these distributions.

and then immersed in 70% ethanol (for around 2 min) in a 24-well plate. The successful implantation of silver was functionally validated by the significant antibacterial effects described in the Results section. Direct surface chemical analysis on these specific, complex-geometry implants was not feasible with our available equipment; this presents a valuable direction for future research using advanced, tailored characterisation techniques. The samples were then transferred to a fresh well plate and allowed air dry before characterisation and biological evaluation.

### Bacterial growth

Before each bacterial attachment experiment, *S. aureus* NCTC 7791 (Culture Collections, UK Health Security Agency, UK) bacterial cultures were prepared from a single colony on tryptone soya agar (TSA) and grown overnight in tryptone soya broth (TSB) at 37°C, 5% $CO_2$.

Overnight bacterial culture (10 ml) was transferred to a universal container and centrifuged at 5000 g for 5 min. The bacterial pellet was then resuspended with phosphate buffered saline (PBS) and centrifuged again at 5000 g for 5 min. The pellet was resuspended in PBS to an optical density (OD600 nm) of 0.09–0.10 (corresponding to approximately $1 \times 10^7$ CFU/ml).

### Bacterial retention study

The LCP specimen exhibits intricate geometrical characteristics, including multiple surface curvatures. In alignment with established engineering methodologies that advocate preliminary coupon testing, regions with minimal surface curvature were identified and segmented into 0.5 × 0.5 cm subcomponents. These subcomponents were subsequently bisected to create stable base sections, thereby ensuring that the treated surface would face upward.

A 15 µl droplet of the inoculum was added to each sample surface in a 24-well plate and incubated for 1 hour at 37 °C, 5% $CO_2$. The samples were then transferred to a fresh 24-well plate and washed in 1 ml of 0.85% NaCl. Live/dead staining was performed according to the manufacturer's instructions (LIVE/DEAD BacLight Viability Kit, Thermofisher Scientific, UK) and imaged using an AX-70 fluorescent microscope (Olympus, Japan) at magnifications of ×10, ×20 and ×40. The percentage area coverage or bacterial coverage (BC) was quantified using ImageJ software as outlined in a previous publication[33] from the ×10 magnification images to ensure the largest sample surface area was analysed. Due to the complex topography of the LCP samples, it was necessary to analyse multiple representative in-focus regions per sample. While this provides a robust estimate, we acknowledge that techniques such as confocal laser scanning microscopy, which can construct a 3D image from optical sections, would provide a more comprehensive and accurate quantification for future studies on such geometries.

### Osteoblast-like cell culture, attachment and morphology

To assess the biocompatibility/cytotoxicity of the manufactured surfaces, human MG-63 osteoblast-like cells (Sigma Aldrich, UK) were used. Cell attachment was studied to determine how chemical modification might affect bone formation, and cell morphology was studied to determine whether surface chemical modification may induce cytoskeletal changes and therefore influence osteogenic potential. Cells (passages 29–32) were seeded at 5000 cells/$cm^2$ and maintained in T75 cell culture flasks in culture medium comprising of alpha minimum essential medium (α-MEM) supplemented with 10% (v/v) heat-inactivated foetal bovine serum (FBS) and 100 units/mL penicillin G sodium, 0.1 µg/ml streptomycin sulphate and 0.25 µg/ml amphotericin (Thermofisher Scientific, UK). The cells were incubated at 37 °C, 5% $CO_2$, and the medium was changed every 2–3 days. Cells were cultured until they reached approximately 80%–90% confluency before being used for subsequent experiments.

The cells were detached using trypsin-EDTA, counted and seeded directly on the control surfaces and the Ag ion-implanted surfaces in a 24-well plate at a density of 100 cells/µl (approximately 1500 cells per sample). Samples were incubated for 1 h at 37 °C, 5% $CO_2$ to allow attachment. The wells were then flooded with 500 µl of complete culture media and incubated for a further 24 hours.

Subsequently, the samples were washed three times with PBS to remove non-adherent cells and incubated in 500 µl of 10% formalin overnight at 4 °C to fix the attached cells. Following incubation, the formalin solution was removed, and the samples were washed three times with tris-buffered saline (TBS). The cells were then permeabilised with filtered 1% Triton X-100 (Sigma Aldrich, UK) for 30 min at room temperature. After permeabilisation, the samples were washed three times with TBS. Incubation of the samples for 1 hour at room temperature with a solution of 1% bovine serum albumin (Vector Laboratories, UK) in TBS was performed to block non-specific binding sites. Following incubation, the actin filaments of the cells were stained with freshly prepared fluorescein isothiocyanate (FITC) labelled phalloidin (diluted 1:50 in TBS, Sigma Aldrich, UK) and incubated in the dark for 40 mins at room temperature. The samples were then washed three times with TBS and allowed to air dry for 5 min. Subsequently,10 µl of 4′,6-diamidino-2-phenylindole (DAPI, Vector Laboratories, UK) was added to each sample surface to stain the nuclei of the cells. Images of the cell actin filament and nuclei were taken at magnifications of ×10, ×20, ×40 using an AX70 Olympus fluorescent microscope (Olympus, Japan). FITC and DAPI channels were superimposed using ImageJ. Cell attachment and morphology analysis were performed on fluorescent images.

Similar to the bacterial quantification, cell attachment analysis on these freeform surfaces was challenged by

topography. The qualitative assessment of morphology and relative attachment is clear; however, precise quantitative analysis would be enhanced in future work by using 3D surface scanning to normalise counts to actual surface area or by using z-stack imaging via confocal microscopy.

### Surface preparation for SEM bacteria imaging

Following bacterial tests for silver-implanted surfaces, the adhered bacteria were fixed in 10% formalin for 10 min to fix the attached bacteria while retaining their morphologies through protein crosslinking. After that, they were rinsed and dried again for 1 hour, then placed in different concentrations of ethanol for 10 min successively (30%, 50%, 70%, 90% and 100%) and dried in a class 2 flow hood.[8,34] Following submersion in ethanol, the samples were sputter-coated with a 10 nm gold layer to ensure conductivity for SEM imaging. A Tescan S8215G field emission (Tescan, Czechia) scanning electron microscope (FE-SEM) was employed for the visualisation.

### Statistical analysis

Bacterial and cell culture experiments were performed in triplicate for all surfaces. Three images (×10) were taken at random and analysed for each sample.

All data were first assessed for normality using the Shapiro–Wilk test. For normally distributed datasets, one-way analysis of variance (ANOVA) was performed. Where ANOVA indicated statistical significance ($p \leq 0.05$), Tukey's multiple comparison test was applied for post-hoc pairwise comparisons. Data are presented as mean ± standard deviation. Effect sizes (Cohen's *d*) were calculated where relevant to quantify the magnitude of observed differences. A *p* value of ≤ 0.05 was considered significant, whereas in the case of a *p* value of > 0.05, the results were reported as observational. In the case that the ANOVA-obtained *p* value was found to be less than 0.05, Tukey's multiple comparisons test was performed to obtain pairwise comparisons between data means. GraphPad Prism (Boston, USA) was used for the analysis. All data were expressed as the mean accompanied by the standard deviation. For statistically significant results ($p \leq 0.05$), the effect size was calculated using Cohen's *d* to quantify the magnitude of the difference between groups.

## Results

Silver ion surface treatment was conducted on three different types of implants, each having a different material composition as outlined in the methods section. The implants are shown before and after the surface treatment in Figure 3. Focusing on fracture fixation applications, the scope of the experimental investigation was confined to stainless-steel LCP samples.

It was not possible in this instance to conduct detailed and high-resolution chemical analysis of these surfaces. However, the Stopping Range of Ions in Matter (SRIM) simulations[35] were applied in order to gain insights into the depth of implantation of silver in the bulk stainless-steel material of the LCP samples.

It must be emphasised that SRIM simulations represent an idealised model assuming flat, homogeneous substrates and normal incidence ion trajectories. These assumptions inherently limit their predictive power when applied to full-scale orthopaedic implants with freeform geometries.

The SRIM simulation graph in Figure 4 demonstrates a distinct profile of silver ion concentration as a function of implantation depth in stainless steel. The concentration of silver ions exhibits a peak at a depth of 13 nm beneath the implant surface, indicating the maximum penetration of ions achieved through the implantation process. Beyond this peak, the concentration decreases gradually, suggesting a diffusion-controlled penetration of silver ions into the stainless-steel substrate with the presence of silver at a maximum depth of 33 nm.

SEM micrographs in Figure 5a and 5b show fewer *S. aureus* cells attached to Ag-treated LCPs compared to controls. Representative fluorescence micrographs illustrating the antibacterial efficacy and cellular response are presented in Figure 5c–5f. These micrographs provided a clear visual corroboration of the quantitative data. Live/Dead staining showed dense bacterial biofilms on control surfaces, contrasted by sparse, predominantly dead colonies on Ag-treated implants, as shown in Figure 5c and 5d. Furthermore, staining of MG-63 cells revealed healthy, spread morphologies on controls, while Ag-treated surfaces exhibited significantly fewer cells with a rounded, non-adherent morphology (Figure 5e and 5f). Also, the number of cells attached to the untreated stainless-steel implant surface was higher than the number of cells attached to the Ag-treated surfaces. Additionally, the cells seem to be presenting a healthier morphology and attachment to the untreated surfaces compared to the Ag-treated surfaces.

The silver-treated LCP samples showed a significantly reduced BC compared to the control LCP ($p < 0.01$, Cohen's $*d* = 8.2$), while the percentage of dead bacteria was significantly higher on the Ag-treated surfaces ($p < 0.001$, Cohen's $*d* = 10.6$) (Figure 6). These very large effect sizes indicate a substantial and meaningful biological effect of the silver treatment.

## Discussion

The SRIM simulations indicate variations in silver ion distribution within the stainless-steel orthopaedic implants, especially when considering the unique challenges presented by freeform surfaces. Unlike the uniform distribution expected in theoretical models or simulations tailored for flat surfaces,

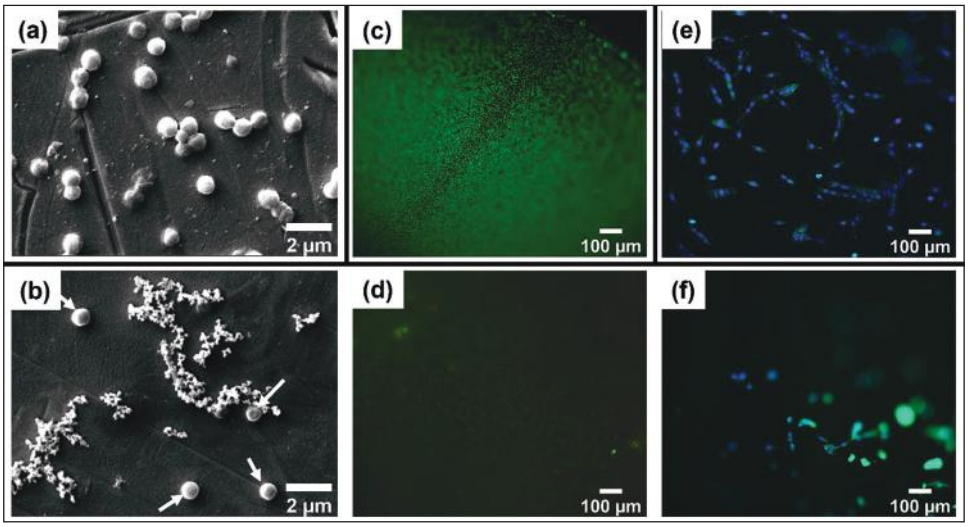



**Figure 5.** Scanning electron microscope (SEM) images of *S. aureus* on (a) control and (b) silver-treated LCP samples. White arrows indicate attached bacteria. Fluorescence microscopy images of *S. aureus* (Live/Dead stain) on (c) control and (d) silver-treated LCP samples. Fluorescence microscopy images of MG-63 osteoblast-like cells (Phalloidin/DAPI stain) on (e) control and (f) silver-treated LCP samples.

the intricate geometries of the tested implants suggest a more complex implantation dynamic. This complexity is particularly evident in the context of surface treatments aimed at enhancing antibacterial properties through silver ion implantation. The simulations predict a heterogeneous distribution of silver ions, which might not directly correlate with a uniform enhancement of antibacterial efficiency across the entire surface of the implants. Although the SRIM results provide valuable insights into the potential distribution of silver ions, the actual antimicrobial efficacy of these treated surfaces would likely be influenced by the specific surface geometries and the resulting variation in ion concentration at different locations.

In this study, the SRIM simulations were conducted by feeding the software details about the composition of the target material, in this case, the LCP material, the ion energy, the implanted/impregnated material (silver) and the angle of incidence (normal incidence).

A limitation of this study on full-scale implants is the lack of direct surface chemical characterisation (e.g., XPS, TOF-SIMS) to quantify the silver concentration, depth profile and chemical state. As noted, this was due to the significant technical challenge of analysing large, non-planar and intricately shaped objects with standard surface science equipment, which is typically designed for flat, small coupons. Consequently, we relied on SRIM simulations for a theoretical depth profile and, most importantly, on functional biological assays to confirm the implantation's efficacy. The significant antibacterial results shown in Figure 6 provide strong indirect evidence that silver was successfully implanted and is biologically active. The observed discrepancy between our results and the literature for flat samples underscores the fact that without direct characterisation, it is difficult to deconvolute the precise effect of geometry on the ionic distribution. Therefore, we explicitly state that future work must prioritise overcoming these characterisation hurdles, potentially through the use of destructively sectioning implants or developing new analytical protocols for complex shapes, to directly link implantation parameters on freeform surfaces to biological outcomes.

The decreased bacterial attachment could be an indication that silver ions actively kill bacteria in the solution, decreasing the number of live bacteria seeking attachment. It has indeed been documented that Ag ion implantation acts better on free-floating bacteria, as in this state, the $Ag^+$ ions can easily interact with the bacteria.[36] A key methodological challenge in this study was the accurate quantification of biological response on the complex freeform surfaces of the clinical implants. Standard epifluorescence microscopy, used here, has a limited depth of field, meaning only portions of the curved LCP surface could be in-focus at one time. This required analysis of multiple representative in-focus regions, a method which, while providing a good estimate, introduces potential for selection bias and may under-represent the total surface area. Advanced techniques such as confocal laser scanning microscopy (which can compile z-stacks into a 3D image) or 3D surface profilometry (to map topography and correct fluorescence counts for real surface area) would provide superior quantification. Despite this limitation, the qualitative results are unequivocal: a stark contrast in BC and cell density is visually apparent between Ag-treated and control surfaces across all replicates. The quantitative data presented, therefore, should be interpreted as a robust *relative comparison* between treatment groups, rather than an absolute measure of total coverage.

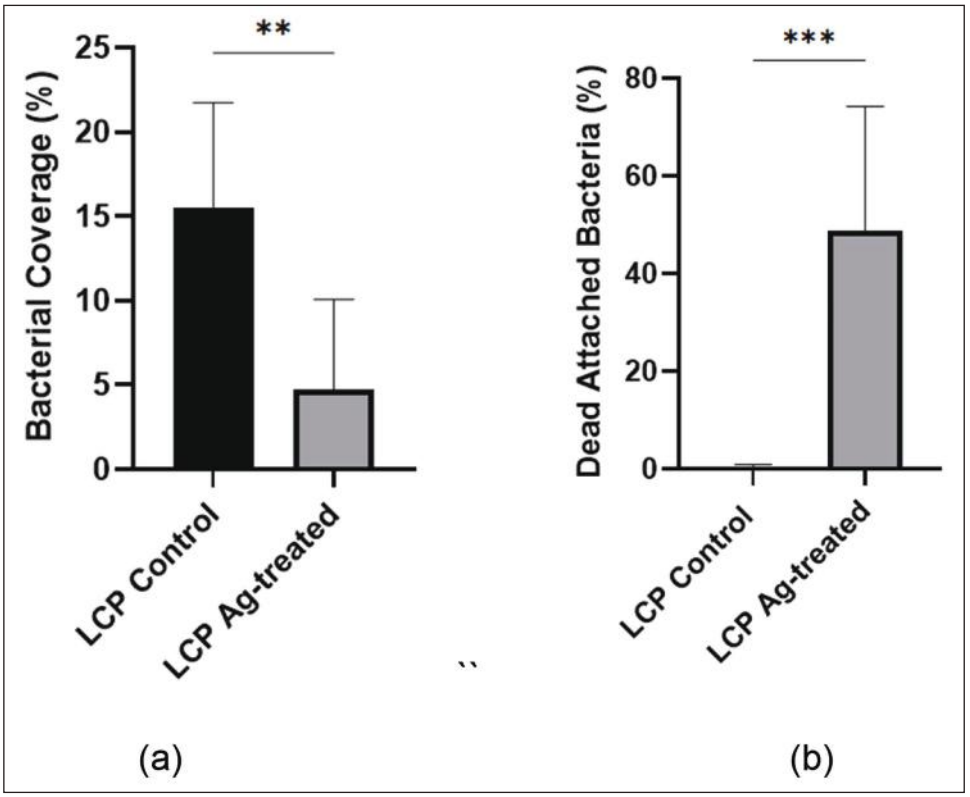



**Figure 6.** (a) The bacterial coverage on both LCP control and Ag-treated samples. (b) The percentage of dead bacteria attached to the surface of LCP control and Ag-treated samples. Statistical significance was determined using one-way ANOVA with Tukey's *post-hoc* test. $^{**}p < 0.01$, $^{***}p < 0.001$. The calculated Cohen's *d* effect sizes for the differences are 8.2 and 10.6, respectively, indicating an extremely large magnitude of effect.

Beyond the antibacterial efficacy, a key finding of this study is the observed reduction in osteoblast-like cell (MG-63) attachment and spreading on the silver-treated surfaces, as evidenced by their rounded morphology (Figure 5f). This has important and nuanced clinical implications for implant stability and healing. For permanent implants, such as joint arthroplasties, this would be a significant concern, as strong osseointegration is essential for long-term stability and load-bearing function. However, the context of the implant's purpose is critical. LCPs and other fracture fixation devices are primarily temporary implants, designed to provide mechanical support only until the bone has healed, after which they are often removed. In this specific application, the clinical paradigm is different. Excessive osseointegration is a well-documented complication, making removal surgery difficult, requiring extensive dissection, and increasing the risk of re-fracture, operative time, and patient morbidity.

Therefore, the observed inhibition of osteoblast function, while a drawback for permanent implants, can be reinterpreted as a potential *benefit* for temporary fracture fixation devices. A surface that actively resists strong bone ingrowth could significantly simplify future removal procedures. This positions silver ion implantation not as a universal coating, but as a promising strategy for a specific implant class where the primary clinical challenges are infection prevention and the facilitation of easier removal, without completely sacrificing the mechanical stability required for the initial healing period. Future studies should aim to quantify this balance between sufficient stability for healing and reduced integration for removal.

As illustrated in Figure 7, the mean antibacterial efficacy of the Ag-treated LCP surfaces in this study is significantly lower than the efficiencies reported in the literature for a similar nominal Ag ion dosage.[32,37–40] This can be quantitatively explained by the complex geometry of the implant. The reduction in efficacy is attributed to two primary geometric effects:

1. Surface Area Shadowing: A commercial LCP is not a flat surface but a complex structure with numerous screw holes, edges, and curved regions. During the PIII process, these features create zones of "self-shielding" where the ion flux is partially or completely blocked. A simple geometric model of our LCP plate estimates that approximately 20%–30% of the total surface area consists of these shielded regions (e.g., the walls of screw holes), which would receive a substantially lower ion dose.

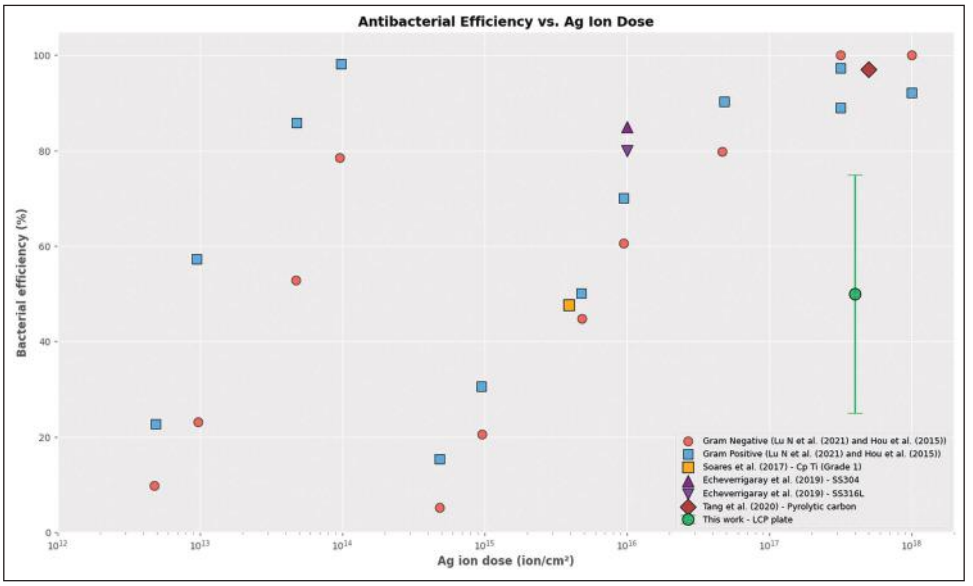



**Figure 7.** The position of the current results within the literature. The significantly lower antibacterial efficacy observed in this study, compared to literature values for flat coupons treated with a similar nominal dose, is attributed to the reduction in effective dose caused by the complex geometry of the freeform LCP implant. Data for the plot were extracted from several sources.[32,37–40]

2. Angular Dependence of Implanted Dose: Ion implantation is most effective at normal incidence (0°). The effective implanted dose decreases as a function of the angle of incidence ($\theta$) relative to the surface normal, following the relation D_eff = D_nominal × cos($\theta$). On a complex geometry like an LCP, a significant portion of the surface is oriented at high angles. For example, a surface at 60° incidence would receive an effective dose of only 50% of the nominal dose (cos(60°) = 0.5), leading to a sub-lethal silver concentration.

Therefore, the nominal dose ($4.0 \times 10^{17}$ ions/cm²) represents a maximum value only achievable on ideal flat surfaces oriented perpendicular to the ion flux. The effective weighted average dose across the entire implant is considerably lower due to shadowing and angular effects. This model robustly explains the discrepancy with flat-sample studies and underscores that process parameters must be optimised for the specific geometry of the target implant to ensure a uniformly bactericidal surface.

This divergence is a central finding and is attributed to the fundamental difference in substrate geometry. The cited studies utilised flat, polished samples, which allow for uniform ion flux and predictable implantation profiles. In contrast, our work on freeform LCP surfaces reveals that complex geometries lead to varied angles of incidence and potential shadowing effects, resulting in a non-uniform distribution of implanted silver ions. This heterogeneity likely explains the observed reduction in overall antibacterial performance compared to idealised flat surfaces.

The distinction in antibacterial efficiency between the implants studied and those reported in literature for similar Ag ion dosages draws attention to the impact of surface geometry on treatment effectiveness. The expected ion concentration and distribution on freeform surfaces such as LCP may differ from those on flat samples, potentially explaining the variations in observed antimicrobial performance. This discrepancy suggests that the specific conditions and characteristics of the implantation process, as well as the surface to be treated, play crucial roles in determining the final antibacterial efficacy of silver-ion-implanted/impregnated surfaces.

## Conclusions

This study investigated the application of silver ion implantation on full-scale orthopaedic LCP implants to explore its potential for antimicrobial activity against *S. aureus*. Our experimental findings showed a statistically significant 72% reduction in bacterial attachment and a 4.5-fold increase in dead bacteria on silver-impregnated surfaces, compared to controls. Additionally, osteoblast attachment was reduced by over 60%, indicating that while antimicrobial properties are enhanced, osseointegration is correspondingly suppressed.

This study demonstrates that the antibacterial performance of silver ion implantation, previously established on flat samples, is significantly challenged by the complex geometries of real-world orthopaedic implants. The observed deviations from results on flat surfaces are not simply experimental error but are a direct consequence of freeform topography. Therefore, the primary conclusion of this work is that

optimisation of surface engineering techniques, such as PIII must be conducted on clinically relevant geometries to be truly predictive of clinical performance.

The difference between the results obtained for flat surfaces from existing literature and the freeform surfaces in this study highlighted the need for further research and optimisation of the implantation process on intricate surfaces. This need is also coupled with the requirement for in-depth chemical analysis of surfaces to determine implantation depth and concentration more accurately.

Moreover, the study observed a reduction in osteoblast cell attachment and spreading on silver-treated surfaces. This outcome suggests that while silver ion implantation may enhance antimicrobial properties, it could also influence osseointegration processes. Notably, this reduction in osteoblast activity may facilitate future removal of the implants, given that certain orthopaedic fixtures, including LCPs, are intended for eventual extraction after fulfilling their temporary role in supporting bone healing.

This study also underscored the significant challenges in imaging and quantifying biological data on freeform surfaces using traditional microscopy. Future work must adopt advanced methodologies, such as confocal laser scanning microscopy and 3D surface scanning, to overcome the limitations of depth of field and to normalise data to the true surface area, thereby enabling absolute quantification on complex implant geometries.

In summary, while the promising antibacterial activity of silver-ion-treated surfaces was evidenced, future work must overcome the challenges of surface chemical analysis on complex geometries (e.g., via destructive cross-sectioning and analysis of representative areas) to precisely quantify silver concentration and distribution. This will allow for the adaptation and optimisation of implantation strategies for freeform surfaces to fully exploit the potential of silver ion implantation in orthopaedic applications. These findings highlight the need to tailor surface micromanufacturing approaches specifically for temporary fracture fixation implants, where both infection control and ease of removal are critical clinical requirements.

## Declaration of Conflicting Interests

The authors declared no potential conflicts of interest with respect to the research, authorship and/or publication of this article.

## Funding

The authors disclosed receipt of the following financial support for the research, authorship, and/or publication of this article: This work was funded by the UKRI via Grant No. EP/T024607/1, Cambridge Royce facilities grant EP/P024947/1 and Sir Henry Royce Institute - recurrent grant EP/R00661X/1, the Hubert Curien Partnership award 2022 from the British Council and the International exchange Cost Share award by the Royal Society (IEC\NSFC\223536). The contribution of J.C., R.B. and J.O. (Eurecat) has been financed by the Ministry of Science and Innovation of Spain under the project BIOIMPLANT (RTC2019-006803-1) and DEMANDING (PGC2018-096855-B-C42). Funding from the Spanish Agencia Estatal de Investigación (Projects PID2021-128727OB-I00 and TED2021-132752B-I00) is also acknowledged.

## Supplementary Material

Supplementary material for this article is available online.

## ORCID iD

Saurav Goel https://orcid.org/0000-0002-8694-332X

## References

1. Anantavorasakul N, Lans J and Wolvetang NH. Forearm plate fixation: Should plates be removed? *Arch Bone Jt Surg* 2022; *10*(2): 153.
2. Katzer A and Lœhr J. Early loosening of hip replacements: Causes, course and diagnosis. *J Orthop Traumatol* 2003; *4*: 105–116.
3. Patel KH, Gill LI, Tissingh EK, et al. Microbiological profile of fracture related infection at a UK major trauma centre. *J Bone Jt Infect* 2023; *12*(9): 1358.
4. Iliaens J, Onsea J, Hoekstra H, et al. Fracture-related infection in long bone fractures: A comprehensive analysis of the economic impact and influence on quality of life. *Injury* 2021; 52(11): 3344–3349.
5. Chen X and Schluesener HJ. Nanosilver: A nanoproduct in medical application. *J Toxicol Lett* 2008; *176*(1): 1–12.
6. Wafa H, Grimer R, Reddy K, et al. Retrospective evaluation of the incidence of early periprosthetic infection with silver-treated endoprostheses in high-risk patients: Case-control study. *Bone Jt J* 2015; *97*(2): 252–257.
7. Jin G, Qin H, Cao H, et al. Synergistic effects of dual Zn/Ag ion implantation in osteogenic activity and antibacterial ability of titanium. *Biomaterials* 2014; 35(27): 7699–7713.
8. Hawi S, Goel S, Kumar V, et al. Precision laser manufacturing and metrology of nature-inspired bioactive surfaces for antibacterial medical implants. *Surf Interfaces* 2025; *62*: 106267.
9. Hawi S, Goel S, Kumar V, et al. Critical review of nanopillar-based mechanobactericidal systems. *ACS Appl Nano Mater* 2022; *5*(1): 1–17.
10. Hirvonen JK. *Treatise on materials science and technology: Ion implantation*. London: Academic Press, 1980.
11. Kroner F, Schork R, Frey L, et al. Phosphorus ion shower implantation for special power IC applications. *In: 2000 international conference on ion implantation technology proceedings. Ion implantation technology-2000 (cat. no. 00EX432)*. New York: IEEE, *2000*, pp.476–479.
12. Conrad JR, Radtke JL, Dodd RA, et al. Plasma source ion-implantation technique for surface modification of materials. *J Appl Phys* 1987; *62*(11): 4591–4596.
13. Anders A. From plasma immersion ion implantation to deposition: A historical perspective on principles and trends. *Surf Coat Technol* 2002; *156*(1–3): 3–12.
14. JMatsuo J, Aoki T and Seki T. Cluster ion implantation—prospects and challenges. In: *2007 international workshop on junction technology*. New York: IEEE, *2007*, pp.53–54.
15. Gotoh Y, Tsuji H and Ishikawa J. Molecular ion implanter equipped with liquid-metal alloy ion source. *Rev Sci Instrum* 2000; *71*(2): 780–782.

16. Gupta D. Plasma immersion ion implantation (PIII) process—physics and technology. *Int J Adv Technol* 2011; *2*(4): 471–490.
17. Larrañaga-Altuna M, Zabala A, Llavori I, et al. Bactericidal surfaces: An emerging 21st-century ultra-precision manufacturing and materials puzzle. *Appl Phys Rev* 2021; *8*(2): 021303.
18. Miller AC, Rashid RM, Falzon L, et al. Silver sulfadiazine for the treatment of partial-thickness burns and venous stasis ulcers. *J Am Acad Dermatol* 2012; *66*(5): e159–e165.
19. Arendsen LP, Thakar R and Sultan AH. The use of copper as an antimicrobial agent in health care, including obstetrics and gynecology. *Clin Microbiol Rev* 2019; *32*(4): DOI: 10.1128/cmr.00125-18
20. Lopez S, Hallali N, Lalatonne Y, et al. Magneto-mechanical destruction of cancer-associated fibroblasts using ultra-small iron oxide nanoparticles and low frequency rotating magnetic fields. *Nanoscale Adv* 2022; *4*(2): 421–436.
21. Kirthika S, Goel G, Matthews A, et al. Review of the untapped potentials of antimicrobial materials in the construction sector. *Prog Mater Sci* 2023; *133*: 101065.
22. Ahmad SA, Das SS, Khatoon A, et al. Bactericidal activity of silver nanoparticles: A mechanistic review. *Mater Sci Energy Technol* 2020; *3*: 756–769.
23. Orrit-Prat J, Bonet R, Rupérez E, et al. Bactericidal silver-doped DLC coatings obtained by pulsed filtered cathodic arc co-deposition. *Surf Coat Technol* 2021; *411*: 126977.
24. Qin H, Cao H, Zhao Y, et al. Antimicrobial and osteogenic properties of silver-ion-implanted stainless steel. *ACS Appl Mater Interfaces* 2015; *7*(20): 10785–10794.
25. Ribeiro M, Monteiro FJ and Ferraz MP. Infection of orthopedic implants with emphasis on bacterial adhesion process and techniques used in studying bacterial–material interactions. *Biomatter* 2012; *2*(4): 176–194.
26. Pietrocola G, Campoccia D, Motta C, et al. Colonization and infection of indwelling medical devices by *Staphylococcus aureus* with an emphasis on orthopedic implants. *Int J Mol Sci* 2022; *23*(11): 5958.
27. Mei S, Wang H, Wang W, et al. Antibacterial effects and biocompatibility of titanium surfaces with graded silver incorporation in titania nanotubes. *Biomaterials* 2014; *35*(14): 4255–4265.
28. Kim DS, Kim YM, Choi ES, et al. Repeated metal breakage in a femoral shaft fracture with lateral bowing—a case report. *J Korean Fract Soc* 2012; 25(2): 136–141.
29. Wheeless CR. Spiral blade. *Wheeless' Textbook of Orthopaedics*. Available at: https://www.wheelessonline.com/joints/spiral-blade/ (accessed 2 September 2025).
30. Angerame MR, Jennings JM, Holst DC, et al. Management of bone defects in revision total knee arthroplasty with use of a stepped, porous-coated metaphyseal sleeve. *JBJS Essent Surg Tech* 2019; *9*(2): e14.
31. Pardo A, Buijnsters JG, Endrino JL, et al. Effect of the metal concentration on the structural, mechanical and tribological properties of self-organized aC: Cu hard nanocomposite coatings. *Appl Surf Sci* 2013; *280*: 791–798.
32. Tang H, Liu T, Liu X, et al. A study on biocompatibility and bactericidal properties of pyrolytic carbon by silver ion implantation. *Nucl Instrum Methods Phys Res B* 2007; *255*(2): 304–308.
33. Ayre WN, Scott T, Hallam K, et al. Fluorophosphonate-functionalised titanium via a pre-adsorbed alkane phosphonic acid: A novel dual action surface finish for bone regenerative applications. *J Mater Sci Mater Med* 2016; *27*: 1–12.
34. Rajab FH, Liauw CM, Benson PS, et al. Picosecond laser treatment production of hierarchical structured stainless steel to reduce bacterial fouling. *Food Bioprod Process* 2018; *109*: 29–40.
35. Ziegler JF and Biersack JP. The stopping and range of ions in matter. In: *Treatise on heavy-ion science: Volume 6: Astrophysics, chemistry, and condensed matter*. Berlin: Springer, *1985*, pp.93–129.
36. Sukhorukova I, Sheveyko A, Shvindina N, et al. Approaches for controlled Ag+ ion release: Influence of surface topography, roughness, and bactericide content. *ACS Appl Mater Interfaces* 2017; *9*(4): 4259–4271.
37. Hou X, Mao D, Ma H, et al. Antibacterial ability of Ag–TiO2 nanotubes prepared by ion implantation and anodic oxidation. *Mater Lett* 2015; *161*: 309–312.
38. Lu N, Chen Z, Zhang W, et al. Effect of silver ion implantation on antibacterial ability of polyethylene food packing films. *Food Packag Shelf Life* 2021; *28*: 100650.
39. Soares TP, Garcia CSC, Roesch-Ely M, et al. Cytotoxicity and antibacterial efficacy of silver deposited onto titanium plates by low-energy ion implantation. *J Mater Res* 2018; *33*(17): 2545–2553.
40. Echeverrigaray FG, Echeverrigaray S, Delamare APL, et al. Antibacterial properties obtained by low-energy silver implantation in stainless steel surfaces. *Surf Coat Technol* 2016; *307*: 345–351.



https://dspace.org/

# Antibacterial and osseointegration evaluation of silver ion-implanted orthopaedic implants

**Hawi, Sara; Goel, Saurav; Caro, Jaume; Bonet, Raül; Orrit-Prat, Jordi ...**

**2025-11**
Sage
https://doi.org/10.1177/25165984251382378
Hawi S, Goel S, Caro J, et al., (2025) Antibacterial and osseointegration evaluation of silver ion-implanted orthopaedic implants. Journal of Micromanufacturing, Available online 6 November 2025, Article number 25165984251382378

Downloaded from a DSpace repository. https://dspace.org/